Electronic Supplementary Material (ESI) for Analytical Methods.
This journal is © The Royal Society of Chemistry 2017

SUPPLEMENTARY DATA

Hydrophobic silver nanowire membrane for swabbing extraction and in-situ SERS detection of polycyclic aromatic hydrocarbons on toys

Lanlan Xiao, Min Zhang, Zhen Liu, Weiwei Bian, Xiaoli Zhang and Jinhua Zhan*.

Table of contents

16) **Fig.S12** Calibration curve of pyrene based on PTH-Ag NMs by swabbing from the plastic toy.

1) **Table S1** The directives and opinions about PAHs of toys by different countries, regions and international organizations.

Bundesinstitut für Risikobewertung, BfR	
BfR Opinion Nr. 032/2010	Carcinogenic polycyclic aromatic hydrocarbons (PAHs) in consumer products to be regulated by the EU - risk assessment by BfR in the context of a restriction proposal under REACH
BfR Opinion No 051/2009	Polycyclic aromatic hydrocarbons (PAHs) in toys
International Organization for Standardization，ISO	
ISO 8124-3:2010	Safety of toys
European Standard	
EN 71-2	Safety of toys

2) **Table S2** SERS and normal Raman bands of PTH with their assignments. Wavenumbers in cm^{-1}.

SERS	Normal Raman bands	Assignment
367	370	CCC bend, gauche
614	624	C-S stretch, gauche
688	701	C-S stretch, trans
775	783	CH_2 rock, gauche
888	894	CH_2 rock, gauche
1019	1026	C-C stretch, trans
1082	1086	C-C stretch, gauche
1446	1448	C-C stretch, gauche

3) **Table S3** SERS and normal Raman bands of fluoranthene, anthracene and pyrene with their assignments. Wavenumbers in cm^{-1}.

SERS				
fluoranthene	anthracene	pyrene	Raman bands	Assignment
559			563	skeletal stretch
		591	591	skeletal stretch
	753		753	stretch
802			804	C-H stretch
		1065	1065	CH in-plane bend
1104			1115	C-H in-plane deformation
		1238	1244	C-C stretch/C-H in-plane bend
1270			1271	C-H in-plane deformation
	1402		1400	CC stretch/ring stretch
		1406	1406	CC stretch/ring stretch
1423			1424	C-C stretch
1455			1457	C-C stretch
	1557		1557	C-C stretch
		1595	1598	C-C stretch
1608			1611	C-C stretch
		1628	1628	C-C stretch

4) Table S4 The calculated EFs of PAHs.

Reagents	fluoranthene	anthracene	pyrene
Calculated EF	5.75×10^3	6.85×10^3	1.62×10^4

The enhancement factors (EFs) was calculated by following equation:

$$EF = \frac{I_{SERS}}{I_{Raman}} \times \frac{N_{Raman}}{N_{SERS}}$$

$$N_{SERS} = \frac{S_{laser}}{S_0} \cdot C_{sol} \cdot V_{sol}$$

$$N_{Raman} = S_{laser} \cdot H_{laser} \cdot C_{bulk}$$

$$= S_{laser} \cdot H_{laser} \cdot \frac{m_{bulk}/M_{bulk}}{V_{bulk}} = \frac{S_{laser} \cdot H_{laser}}{M_{bulk}} \cdot \rho_{bulk}$$

$$EF = \frac{I_{SERS}}{I_{Raman}} \times \frac{S_{laser} \cdot H_{laser} \cdot \rho_{bulk}/M_{bulk}}{S_{laser} \cdot C_{sol} \cdot V_{sol}/S_0} = \frac{I_{SERS}}{I_{Raman}} \times \frac{H_{laser} \cdot \rho_{bulk} \cdot S_0}{C_{sol} \cdot V_{sol} \cdot M_{bulk}}$$

$$= 1.1 \times 10^4 \cdot \frac{I_{SERS} \cdot \rho_{bulk}}{I_{Raman} \cdot C_{sol} \cdot M_{bulk}}$$

S_{laser} is the effective area of laser spot;

S_0 is the area of the PTH-Ag NMs, 1 cm×1 cm;

H_{laser} is the effective depth of the scattering laser spot volume and here was estimated as 0.22 cm;

C_{sol} is the concentration of the measured solution, mol·L^{-1}.

V_{sol} is the volume of the measured solution, 20 μL;

m_{bulk} is the mass of pure reagents used to measure non-enhanced Raman intensity;

M_{bulk} is the molar mass of pure reagents used to measure non-enhanced Raman intensity, g· mol^{-1};

V_{bulk} is the volume of the measured pure reagents;

ρ_{bulk} is the density of the measured pure reagents.

5) **Fig.S1** UV−Vis spectrum of the prepared Ag nanowires.

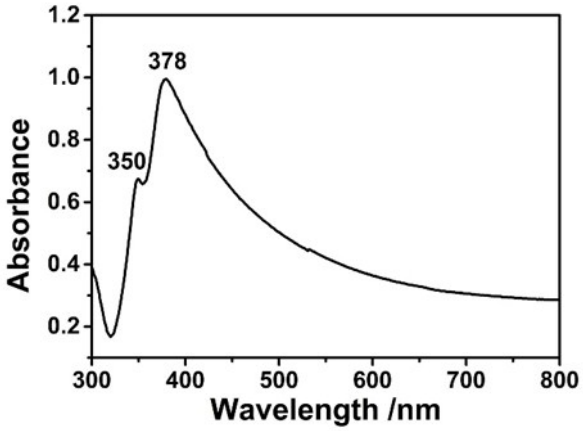

Fig.S1 UV−Vis spectrum of the prepared Ag nanowires.

6) Fig.S2 XRD pattern of silver nanowires.

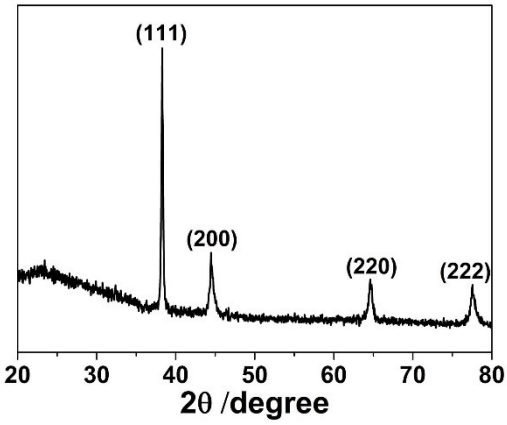

Fig.S2 XRD pattern of silver nanowires.

7) **Fig.S3** The elements on the Ag NMs and PTH-Ag NMs.

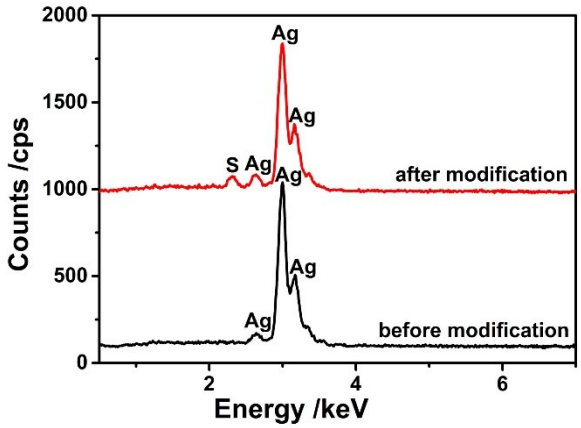

Fig.S3 The elements on the silver nanowire membrane before (red line) and after (black line) the PTH treatment.

8) **Fig.S4** The XPS spectra of Ag NMs and PTH-Ag NMs.

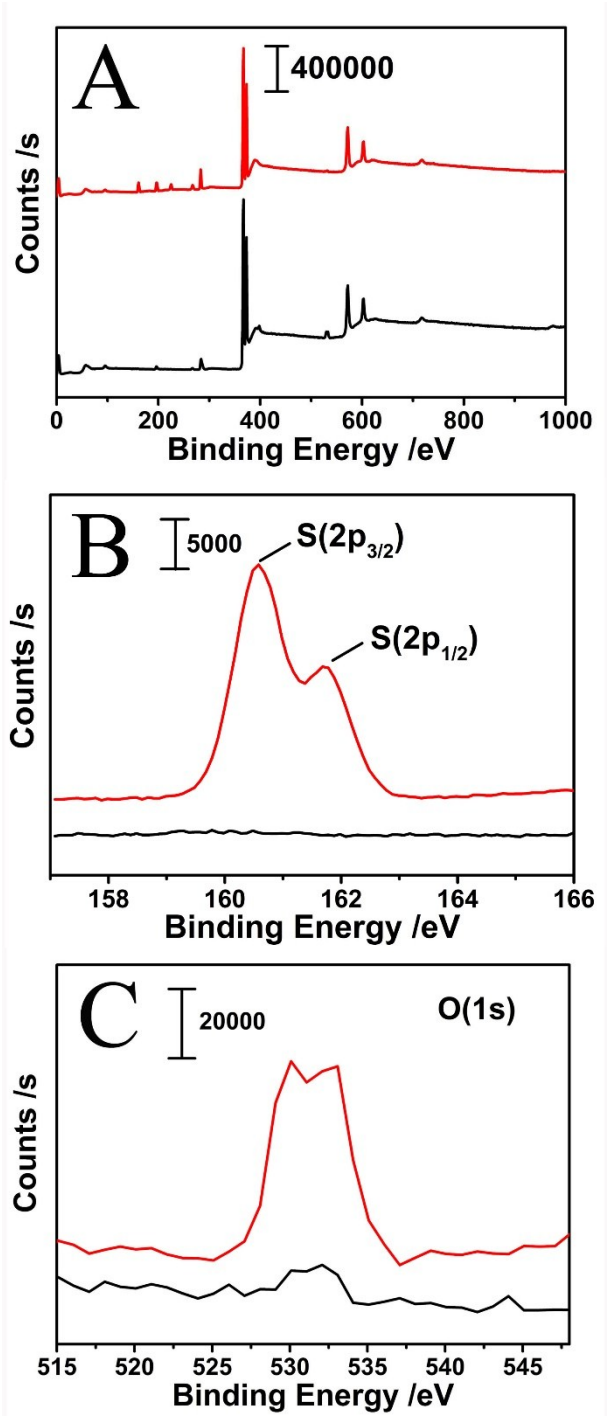

Fig.S4 (A) The XPS spectra of the silver nanowire membrane without (black) and with (red) PTH treatment. (B) XPS spectra of the S (2p) scan of the membrane before (black) and after (red) modification with PTH. (C) XPS spectra of the O (1s) scan of the membrane before (black) and after (red) modification with PTH.

9) **Fig.S5** SERS spectra of fluoranthene on the Ag NMs with different alkanethiol.

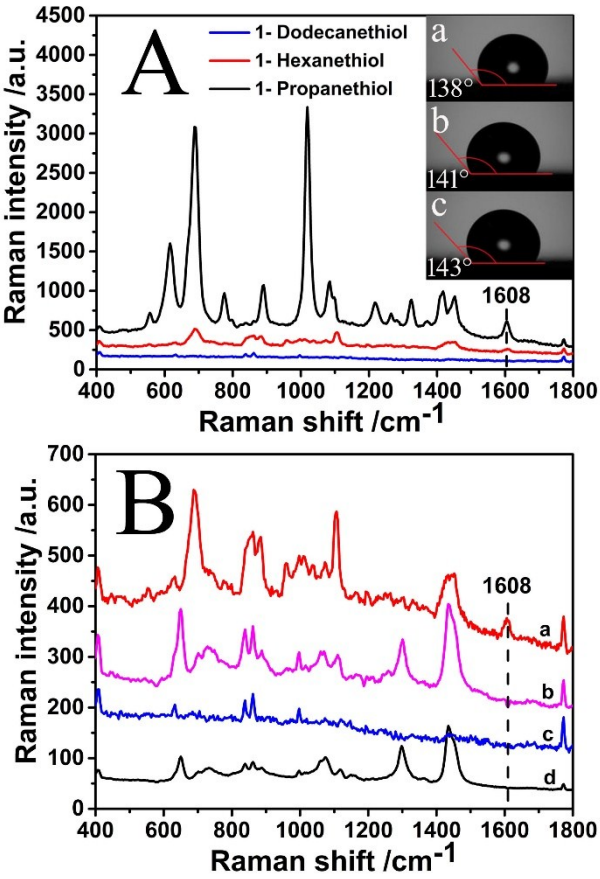

Fig.S5 (A) SERS spectra of fluoranthene (40.45 μg·cm^{-2}) on the Ag NMs with different alkanethiol. The inset shows the static water contact angles of the (a) 10^{-2} M PTH-Ag NMs, (b) 10^{-2} M 1-hexanethiol-Ag NMs and (c) 10^{-2} M 1-dodecanethiol-Ag NMs. (B) The amplified SERS spectra of (a) 10^{-2} M 1-hexanethiol-Ag NMs and (c) 10^{-2} M 1-dodecanethiol-Ag NMs, and the Raman spectrum of (b) liquid 1-hexanethiol and (d) liquid 1-dodecanethiol.

10) **Fig.S6** The influence of PTH concentration on Ag NMs for detecting fluoranthene (40.45 μg·cm^{-2})

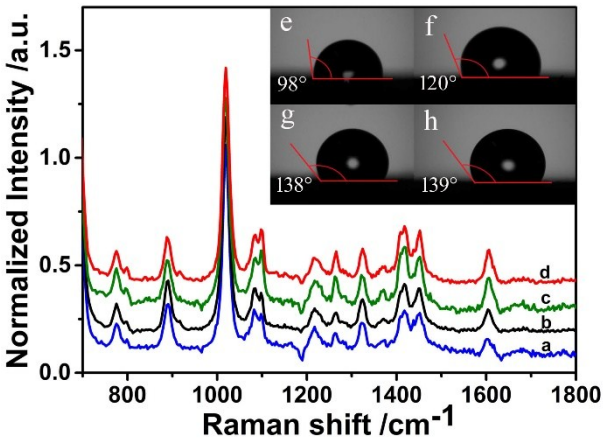

Fig.S6 (A) SERS spectra of fluoranthene (40.45 μg·cm^{-2}) on the PTH-Ag NMs with various concentration of PTH solution (a) 10^{-4} M, (b) 10^{-3} M, (c) 10^{-2} M and (d) 10^{-1} M. (B) The inset shows the static water contact angles of (e) 10^{-4} M PTH-Ag NMs, (f) 10^{-3} M PTH-Ag NMs, (g) 10^{-2} M PTH-Ag NMs, (h) 10^{-1} M PTH-Ag NMs.

11) Fig.S7 Structures of PAHs in this work.

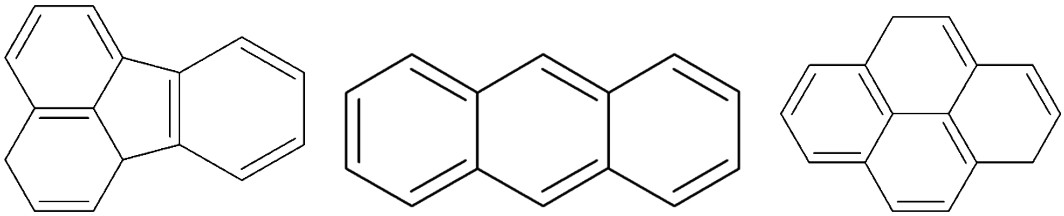

Fluoranthene Anthracene Pyrene

12) Fig.S8 Qualitative analysis of anthracene and pyrene by swabbing from aluminum foil.

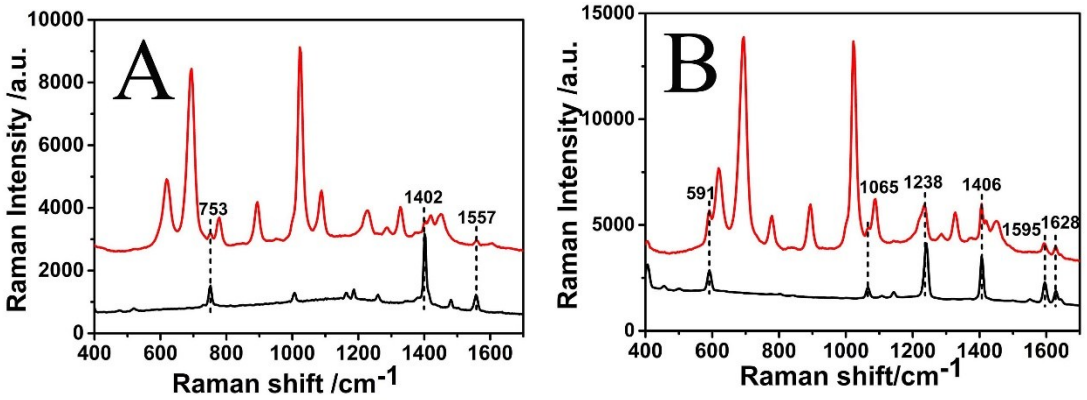

Fig.S8 (A) SERS spectrum of 3.56 μg·cm^{-2} anthracene detected by PTH-Ag NMs (red line) and Raman spectrum of anthracene (black line). (B) SERS spectrum of 4.05 μg·cm^{-2} pyrene detected by PTH-Ag NMs (red line) and Raman spectrum of pyrene (black line).

13) Fig.S9 The reusability of the PTH-Ag NMs.

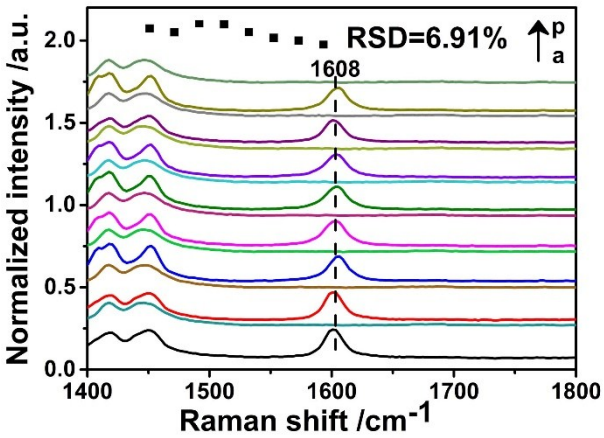

Fig.S9 The reusability of the PTH-Ag NMs. Normalized SERS intensity of fluoranthene (4.04 μg·cm^{-2}) on the Ag nanowire membrane was recorded. (a), (c), (e), (g), (i), (k), (m), (o) was SERS intensity after the 1-8 cycles of swabbing process, respectively. (b), (d), (f), (h), (j), (l), (n), (p) was SERS intensity after the 1-8 cycles of elution process, respectively.

14) Fig.S10 Qualitative analysis of three PAHs by swabbing from plastic toy and rubber toy.

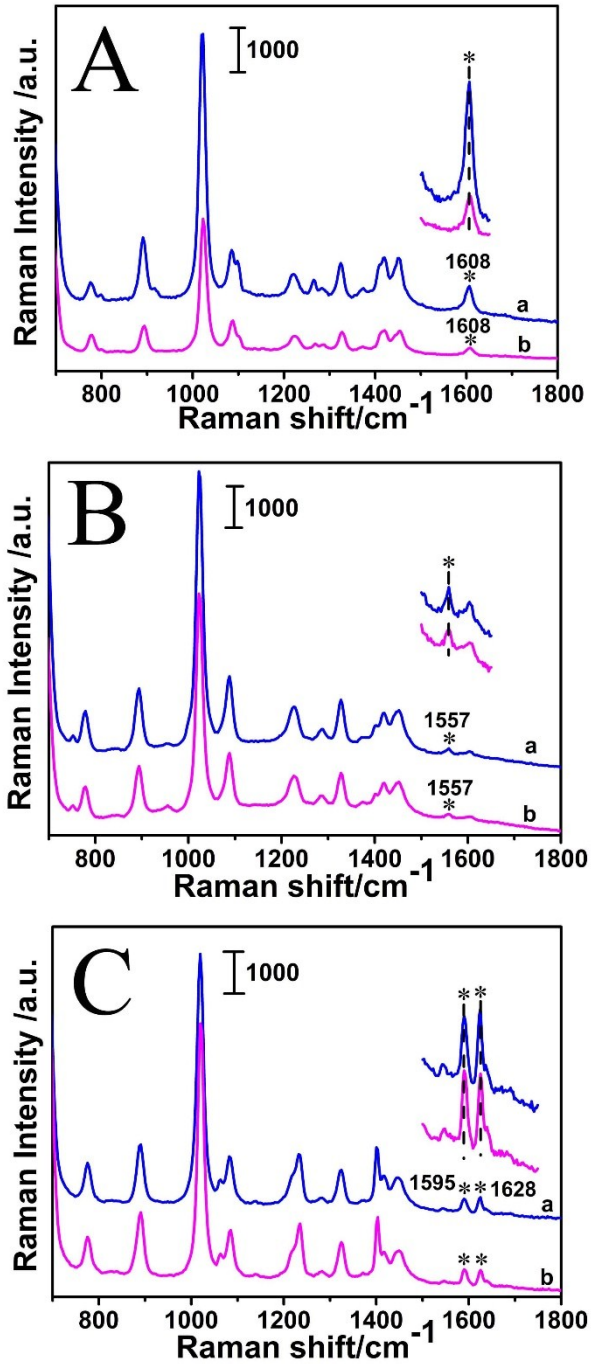

Fig.S10 SERS spectrum of (A) fluoranthene, (B) anthracene and (C) pyrene by swabbing from the surface of (a) the plastic toy and (b) the rubber toy. (A-C) inset: 5 times amplification of the correlative peak.

15) Fig.S11 Quantitative analysis of pyrene by swabbing from plastic toy.

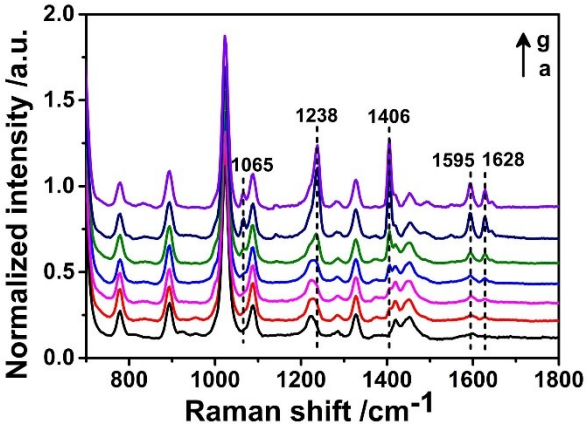

Fig.S11 Normalized SERS intensity of pyrene by swabbing with PTH-Ag NMs. The concentration of pyrene was (a) 40.45 ng·cm^{-2}, (b) 202.3 ng·cm^{-2}, (c) 404.5ng·cm^{-2}, (d) 2023 ng·cm^{-2}, (e) 4045 ng·cm^{-2}, (f) 20225 ng·cm^{-2}, (g) 40450 ng·cm^{-2}.

16) Fig.S12 Calibration curve of pyrene based on PTH-Ag NMs by swabbing from plastic toy.

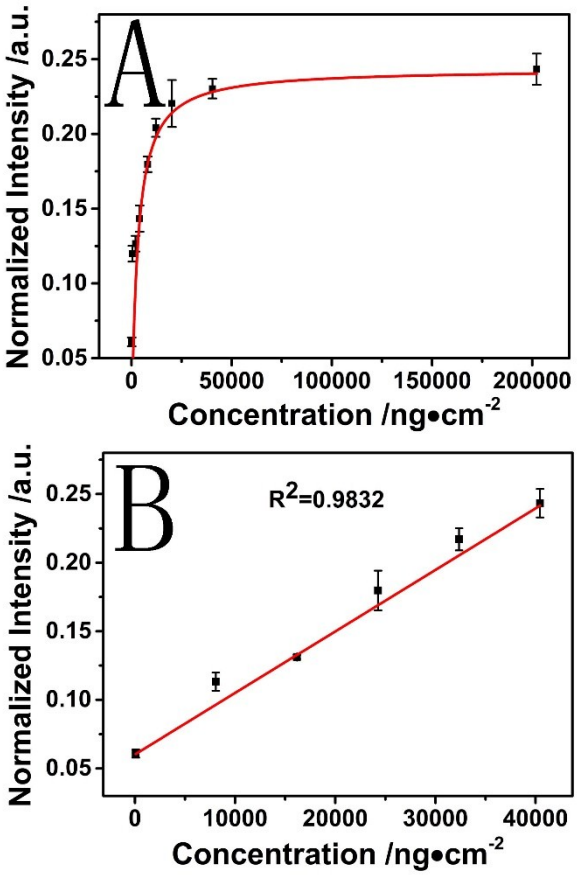

Fig.S12 Quantitative analysis of pyrene by swabbing from the surface of plastic toy. (A) Calibration curve of pyrene based on PTH-Ag NMs. (B) linear fitting of pyrene. The data points correspond to the average of three times parallel measurements.